

PERFORMANCE ANALYSIS OF A MULTICARRIER PACS SYSTEM

Melbourne Barton and Daniel Wong
Telcordia Technologies (formerly Bellcore)
331 Newman Springs Road,
Red Bank, NJ 07701, USA

Abstract

Personal access communications system (PACS) is a 2 GHz band personal communications services (PCS) standard that supports 32 kbps wireless access services for fixed and mobile subscribers. This paper presents a physical layer architecture, and evaluates the performance, of a multicarrier PACS (MPACS) system based on a combination of orthogonal frequency division multiplexing (OFDM) and time division multiple access (TDMA) technologies. It supports nominal user data rates of 32-256 kbps at distances beyond the current range of PACS. For shorter ranges, higher-speed extensions up to 768 kbps are incorporated in the design.

1 Introduction

Personal access communication system (PACS) [1], [2] is a low complexity radio technology designed for interoperable wireless access using both licensed and unlicensed spectrum in the 2 GHz personal communications services (PCS) frequency band. PACS is optimized for operation in multipath fading environments where the root-mean-square (RMS) delay spread does not exceed approximately a 1/4 symbol duration (about 1.25 μ s).

In this paper we develop a multicarrier PACS (MPACS) system design that is robust to multipath fading even where the RMS delay spread extends beyond the PACS symbol duration. It has the following main characteristics: i) same TDMA frame format as PACS, ii) same radio frequency (RF) channel structure as PACS, iii) some modifications to the protocol format, iv) use of 4-, 16- and 64-quadrature amplitude modulation (QAM) on each subcarrier, in addition to the 4-level phase modulation used in PACS, and v) use of the discrete Fourier transform (DFT) for subchannel separation. MPACS will be capable of providing high-speed wireless access services at nominal user data rates of 32-256 kbps, with range extension beyond the current range of PACS. For shorter ranges, higher-speed extensions up to 768 kbps are incorporated in the design.

This paper is organized as follows. Section 2 outlines the MPACS physical layer design. Performance analysis is presented in Section 3, and numerical results are presented in Section 4. Conclusions are presented in Section 5.

2 Multicarrier PACS System Model

A block diagram of the baseband model for the MPACS architecture is shown in Figure 1. The number of OFDM subchannels N can range from 60 to 90 for single timeslot (per subscriber) operation, and up to 480 to 720 for multi-timeslot (per subscriber) operation. K of the N subchannels carry data symbols, while the rest carry peak-to-average power ratio (PAR) symbols and pilot recovery symbols (if required). A cyclic prefix is added to the IDFT output to form the

composite input signal to the transmit pulse shaping filter (PSF).

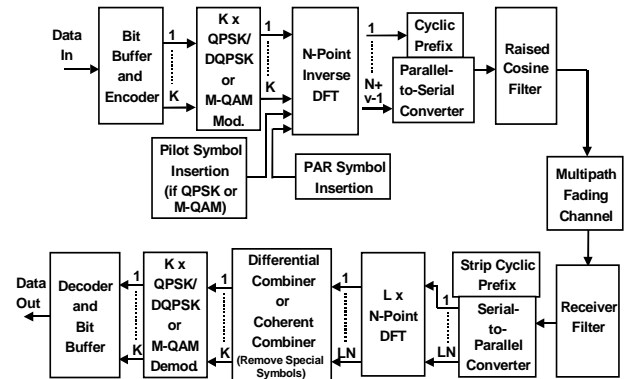


Figure 1. Block diagram of MPACS system model.

At the receiver, an L -branch, e.g., $L=2$, diversity combining technique is used to improve the error rate performance. After receiver signal filtering and removal of the cyclic prefix, the output of the L diversity branches are processed, the frequency-domain PAR symbols and pilot symbols (if any) are removed, and the pilot symbols used for carrier recovery and coherent detection. The remaining sequence of K symbols are demodulated, decoded, and buffered to generate the output data. A simple look-up table has been developed to implement the modulators at the transmitter, and the corresponding demodulators at the receiver. Carrier frequency and timing offset can be derived from the guard interval samples using an integrated estimation algorithm [3].

The physical layer MPACS design incorporates the following. 1) One IDFT per transmitter and one or more DFT's per receiver, depending on the number of diversity branches. 2) Support for quadrature phase-shift keying (QPSK), differential QPSK (DQPSK), $\pi/4$ DQPSK, and 4- to 64-QAM. 3) PAR reduction circuitry. 4) Integrated carrier frequency and timing offset estimation algorithm derived from the precursor guard interval.

2.1 Channel Structure

The N MPACS subchannels are constrained to lie within the 3-dB transmission bandwidth B_C of the MPACS system. If the effective block duration is T_E and the sampling rate $f_s = 1/T$, then $T_E = NT$. Since OFDM is used, the separation between consecutive overlapping subchannels (on adjacent

subcarriers) is $B_s = 1/NT$. Hence the center frequency f_k of the k^{th} subchannel is $f_k = f_0 + k/NT$, for $k \in \{0, N-1\}$.

In the MPACS frame structure, eight timeslots are associated with each 2.5 ms TDMA frame on each RF channel. The MPACS block length $T_s = 312.5 \mu\text{s}$ equals the PACS timeslot. 120 bits are associated with the equivalent single-carrier PACS timeslot in each MPACS block. For QPSK (or $\pi/4$ -QPSK, or 4-QAM) modulation on each subchannel, $K = 60$ subchannels are required. If we assume a single-carrier PACS RF bandwidth of 288 kHz, then the maximum MPACS subchannel bandwidth is $B_s = 4.8$ kHz, the minimum effective MPACS block duration $T_E = 208.33 \mu\text{s}$, and the maximum guard period $T_G = 104.17 \mu\text{s}$. Hence, it is easy to see that $T_G = \alpha T_s$, where α is the roll-off factor for the single-carrier PACS transmit filter. Multi-timeslot operation is simply invoked by increasing the number of subchannels to N times the number of timeslots assigned to each user. Higher user data rates are achieved using multi-level QAM modulation on each subcarrier and timeslot aggregation.

3 Performance Analysis

Let the discrete complex frequency domain symbol $D_i(m)$ denote the output of the m^{th} modulator, with time interval index i . For the i^{th} MPACS block, the IDFT output is given by

$$d_i(k) = \frac{1}{N} \sum_{m=0}^{N-1} D_i(m) e^{j2\pi mk/N}, \quad k = 0, 1, \dots, N-1 \quad (1)$$

The samples $d_i(k)$ form the input to the transmit PSF with impulse response denoted by $h(t)$. v_1 prefix and v_2 postfix samples are added to $d_i(k)$, and the resulting guard interval of $v = v_1 + v_2$ samples added to the MPACS symbol interval. The guard interval is used to eliminate intersymbol interference (ISI) due to inter-block interference (IBI) introduced by the dispersive channel (and symbol clock timing offset, if any). The composite signal at the output of the PSF is given by

$$x(t) = \sum_{i=-\infty}^{\infty} \sum_{l=-v_1}^{N-1+v_2} d_i(l) h(t - lT - i(N+v)T) \quad (2)$$

At the receiver the channel output is sampled at $t = kT$, giving the discrete sampled signal

$$r(kT) = \sum_{m=0}^{M-1} z_m(kT) x(kT - \beta_m T) + w(kT) \quad (3)$$

where $z_m(kT)$ is the complex-valued channel impulse response sample on the m^{th} path at time instant kT , $\beta_m = \tau_m/T$, τ_m is the propagation delay on the m^{th} path, and $w(kT)$ is the additive white Gaussian noise (AWGN) sample. The channel is modeled as a wide-sense stationary (WSS)

uncorrelated scattering Rayleigh fading channel [4] with $z_m(t)$'s that are assumed to be independent WSS narrowband complex Gaussian processes. If the maximum propagation delay τ_{M-1} is such that $\beta_{M-1} \leq v_1$, then no echoes from previous blocks will contribute to interference in the i^{th} block. In general we assume that $\beta_{M-1} < N + v$, so that only the $(i-1)^{\text{th}}$ block will interfere with the i^{th} block. Integer values of β_m are obtained by assuming that within a single chip duration T , individual channel measurement samples are non-resolvable and so are combined to form a single path.

3.1 Signal-to-Interference-to-Noise Ratio Computations

This section develops numerical expressions for estimating the signal-to-interference-to-noise ratio (SINR) of the MPACS system in the presence of: i) inter-channel interference (ICI) due to carrier frequency offset (CFO) and symbol clock timing offset, and ii) IBI due to interference from samples in blocks outside the current decoding interval.

We define the CFO as δ_f , and the quantity $\varepsilon = \delta_f NT$. CFO is modeled as a complex multiplicative distortion of the received data in the time domain, i.e., $e^{j2\pi \varepsilon k/N}$, where ε denotes the difference between the transmitter and receiver oscillators, as a fraction of the subcarrier spacing $1/N$ in normalized frequency. We assume that the received signal is sampled at $t = (k + \Delta)T$, where ΔT is the timing offset. If the guard interval exceeds the total length of the channel impulse response and symbol timing offset, then it provides robustness against coarse symbol timing offset.

Without loss in generality, we normalize the sampling period to $T = 1$. If M_1 paths have propagation delays that are within the precursor guard interval, then from (2), (3) the received signal can be expressed as:

$$r_i(k) = \left\{ \sum_{m=0}^{M_1-1} z_m(k + \Delta) \sum_{l=-v_1}^{N-1+v_2} d_i(l) h(k + \Delta - l - \beta_m) + \sum_{m=M_1}^{M-1} z_m(k + \Delta) \sum_{l=-v_1}^{N-1+v_2} d_i(l) h(k + \Delta - l - \beta_m) u(k - \beta_m) + \sum_{m=M_1}^{M-1} z_m(k + \Delta) \sum_{l=-v_1}^{N-1+v_2} d_{i-1}(l) h(k + \Delta - l - \beta_m + N + v) \bullet (u(k - v_1) - u(k - \beta_m)) \right\} e^{j\frac{2\pi}{N}(k+\Delta)\varepsilon} + w_i(k), \quad \text{for } k = 0, 1, \dots, N-1 \quad (4)$$

where

$$u(k) = \begin{cases} 1, & -v_1 \leq k \leq (N-1+v_2) \\ 0, & \text{elsewhere} \end{cases} \quad (5)$$

Note that the phase term resulting from the carrier frequency and timing offset is absorbed in the AWGN term $w_i(k)$. By

taking the DFT of (4), and using upper case letters to denote DFT, the expression for $R_i(n)$ is given by:

$$R_i(n) = B(n)D_i(n) + C_i(n) + C_{i-1}(n) + W_i(n), \quad (6)$$

$$n = 0, 1, \dots, N-1$$

where $D_i(n)$ is the discrete complex frequency domain symbol at the output of the n^{th} subchannel in the i^{th} decoding block, $B(n)$ is a multiplicative noise term, $C_i(n)$ is the additive ICI term, $C_{i-1}(n)$ is the additive IBI term, and $W_i(n)$ is the AWGN term. It is then easy to show that

$$B(n) = \left\{ \begin{array}{l} M-1 \\ m=0 \end{array} H(n) \hat{Z}_m(-\varepsilon) - \frac{1}{N} \begin{array}{l} M-1 \\ m=M_1 \\ q=0 \end{array} H(n) \hat{Z}_m(-q-\varepsilon) \right. \\ \left. \text{sinc}(q) e^{-j\frac{\pi q}{N}(2\Delta + \beta_m - \nu_1 - 1)} \right\} e^{-j\frac{2\pi n}{N}(\beta_m - \Delta)} \quad (7a)$$

$$C_i(n) = \left\{ \begin{array}{l} M-1 \\ m=0 \\ p \neq n \end{array} H(p) D_i(p) \hat{Z}_m(n - \varepsilon - p) - \frac{1}{N} \begin{array}{l} M-1 \\ m=M_1 \\ p \neq n \\ q=0 \end{array} H(p) D_i(p) \hat{Z}_m(n - \varepsilon - p - q) \right. \\ \left. \text{sinc}(q) e^{-j\frac{2\pi q}{N}(2\Delta + \beta_m - \nu_1 - 1)} \right\} e^{-j\frac{2\pi n}{N}(\rho\beta_m - n\Delta)} \quad (7b)$$

$$C_{i-1}(n) = \frac{1}{N} \begin{array}{l} M-1 \\ m=M_1 \\ p=0 \\ N-1 \\ q=0 \end{array} H(p) D_{i-1}(p) \hat{Z}_m(n - \varepsilon - p - q) \\ \text{sinc}(q) e^{-j\frac{\pi}{N}(q(2\Delta + \beta_m - \nu_1 - 1) + 2p(\beta_m - N - \nu) - 2n\Delta)} \quad (7c)$$

where

$$\hat{Z}_m(n-p) = \frac{1}{N} Z_m(n-p) e^{j\frac{2\pi n \nu_2}{N}} \quad (8a)$$

$$\text{sinc}(q) = \frac{\sin(q\pi(\beta_m - \nu_1)/N)}{\sin(q\pi/N)}. \quad (8b)$$

For large N we assume that the interference terms can be modeled as zero-mean additive complex Gaussian noise, and the average subchannel SINR defined as [5]:

$$\text{SINR} = \frac{E\left(|B(n)D_i(n)|^2\right)}{E\left(|C_i(n)|^2\right) + E\left(|C_{i-1}(n)|^2\right) + E\left(|W_i(n)|^2\right)} \quad (9)$$

where $E(\cdot)$ denotes statistical expectation. An approximate expression for the average subchannel SINR for the n^{th} subchannel is given by:

$$\text{SINR}(n) = \frac{1 - \eta(\varepsilon, \Delta)/\alpha(\varepsilon)}{\left\{ (K(n, \varepsilon) - \eta_1(n, \varepsilon, \Delta))/|H(n)|^2 + \eta(\varepsilon, \Delta) \right\} / \alpha(\varepsilon) - 1 + 1/\text{SINR}(n)} \quad (10)$$

where the average subchannel SNR for the n^{th} subchannel is given by

$$\text{SNR}(n) = \frac{\sigma_D^2 |H(n)|^2}{\sigma_W^2} \alpha(\varepsilon), \quad (11)$$

and σ_D^2 and σ_W^2 are the variance of $D_i(n)$ and $W_i(n)$, respectively. The expressions for the other terms are:

$$\eta(\varepsilon, \Delta) = \frac{1}{M} \begin{array}{l} M-1 \\ m=M_1 \end{array} \left(2 \text{Re}\{\alpha(\varepsilon, \Delta)u(k, \Delta)\} - \alpha(\varepsilon, \Delta)u(k, \Delta)u^*(l, \Delta) \right) \quad (12a)$$

$$\eta_1(n, \varepsilon, \Delta) = \frac{2}{M} \begin{array}{l} M-1 \\ m=M_1 \end{array} \left(\text{Re}\{K(n, \varepsilon, \Delta)u^*(l, \Delta)\} - K(n, \varepsilon, \Delta)u(k, \Delta)u^*(l, \Delta) \right) \quad (12b)$$

$$\alpha(\varepsilon) = \frac{1}{N^2} \begin{array}{l} N-1 \\ k=0 \end{array} \begin{array}{l} N-1 \\ l=0 \end{array} J_0(2\pi f_d(k-l)) \cos(2\pi(k-l)\varepsilon/N) \quad (12c)$$

$$K(n, \varepsilon) = \frac{1}{N} \begin{array}{l} N-1 \\ k=0 \end{array} \begin{array}{l} N-1 \\ l=0 \end{array} J_0(2\pi f_d(k-l)) \varphi_h(k-l) \quad (12d)$$

$$\cos(2\pi(k-l)\varepsilon/N) e^{-j\frac{2\pi}{N}(k-l)n}$$

$$u(k, \Delta) = \frac{1}{N} \begin{array}{l} \beta_m - \nu_1 - 1 \\ r=0 \end{array} \begin{array}{l} N-1 \\ q=0 \end{array} e^{-j\frac{2\pi q}{N}(r-k+\Delta)} \quad (12e)$$

and $\varphi_h(k-l) = \text{IDFT}[|H(p)|^2 e^{-j2\pi p l/N}]$. An average SINR (and SNR) for the MPACS system can be approximated by taking either the arithmetic mean or geometric mean of the subchannel SINR's (and SNR's).

3.2 Bit Error Rate Computations

Diversity combining is included in the receiver to improve the bit error rate (BER) performance. We restrict the analysis to maximum ratio combining (MRC) with L -branch diversity reception [6], and hard decision decoding. The average BER for Gray-coded QPSK and DQPSK modulation with MRC and L -branch receiver diversity is given by [6]:

$$P_b = \frac{1}{2} \left[1 - \rho \begin{array}{l} L-1 \\ l=0 \end{array} \left(\frac{2l}{l} \right) \left(\frac{1 - \rho^2}{4} \right)^l \right] \quad (13)$$

where $\rho = \mu_s / \sqrt{2 - \mu_s^2}$ is the cross-correlation coefficient,

$$\mu_s = \sqrt{\frac{\bar{\gamma}_s}{1 + \bar{\gamma}_s}}, \quad \text{for QPSK}, \quad \mu_s = \frac{\bar{\gamma}_s}{1 + \bar{\gamma}_s}, \quad \text{for DQPSK}, \quad (14)$$

and $\bar{\gamma}_s$ is the average SINR per subchannel. Corresponding results for $\pi/4$ DQPSK modulation with differential detection, and Gray-coded M-QAM constellation are presented in [7].

4 Numerical Results

The numerical results show performance limits for MPACS in the presence of impairments due to ICI, IBI, and/or AWGN on a multipath Rayleigh fading channel. A two-ray channel model approximates the multipath delay spread, with weights that are independent complex Gaussian processes with equal

average powers. The propagation delay of the reflected path $\tau = 2\tau_{RMS}$, where τ_{RMS} is the RMS delay spread. We define an input symbol carrier-to-noise power ratio $CNR = \sigma_D^2 / \sigma_w^2$.

From (11), $SINR(n) = CNR |H(n)|^2 \alpha(\epsilon)$.

Figure 2 and Figure 3 show the SINR performance due to ICI (and AWGN), as a function of Doppler frequency f_D and the number of OFDM subchannels N , for $CNR=30$ dB. The guard interval eliminates IBI, and there is no CFO or symbol clock timing offset. The results in Figure 2 are for single timeslot (per subscriber) operation, with N ranging from 60 to 90, and the maximum number of precursor guard samples v_1 ranging from 30 to 0. Results for multi-timeslot (1-to-8 timeslots per subscriber) operation is shown in Figure 3.

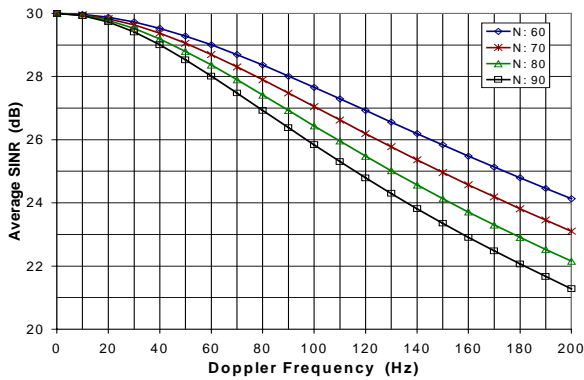


Figure 2. Average SINR performance of MPACS versus f_D , for single timeslot operation, with ICI and AWGN.

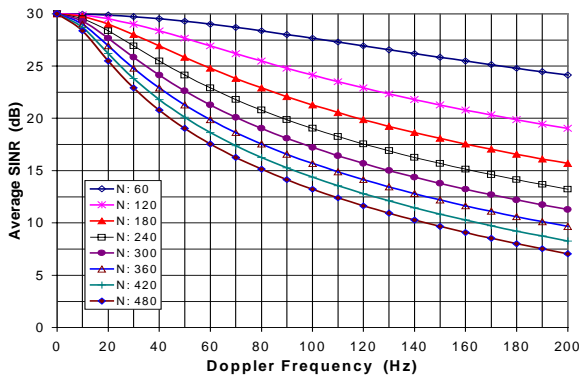


Figure 3. Average SINR performance of MPACS versus f_D , for multi-timeslot operation, with ICI and AWGN.

Figure 4 shows the SINR performance versus CFO when the precursor guard interval is at or below the maximum propagation delay spread. The guard interval is typically about 10% of the block length (i.e., 8 or 9 sampling periods for MPACS). To maintain a reasonable level of SINR performance, the precursor guard interval should be sufficient to eliminate IBI, and the CFO should be limited to approximately 5% of the subchannel bandwidth.

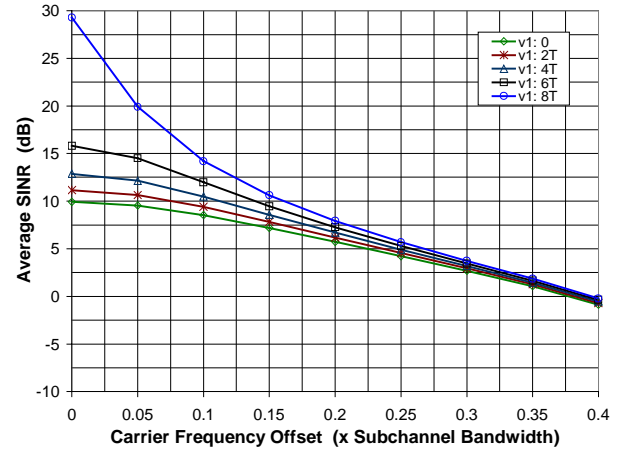


Figure 4. Average SINR performance of MPACS versus CFO, for single timeslot operation and various precursor guard intervals, in the presence of ICI, IBI, and AWGN. $CNR = 30$ dB, $f_D = 20$ Hz, and $\beta_1 = 8$, and timing offset is within one sampling interval.

Figure 5 compares the numerical performance of PACS and MPACS for different fading rates, and RMS delay spread (D) normalized with respect to the PACS symbol interval. The results are for DQPSK modulation with 2-branch diversity and hard decision decoding. For MPACS $v_1 = 8$, CFO is 5% of the subchannel bandwidth, and symbol clock timing offset is within one sampling interval.

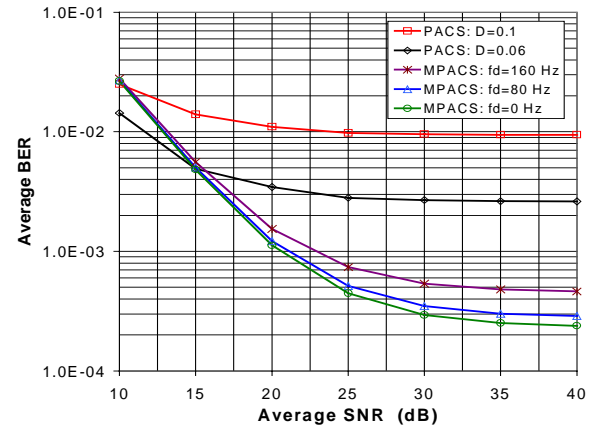


Figure 5. Comparison of average BER performance for PACS and MPACS (for single timeslot operation) with DQPSK modulation, at different normalized RMS delay spread (D) and fading rates (f_D), and 2-branch diversity.

Figure 6 compares the numerical performance of PACS and MPACS as a function of the normalized RMS delay spread. The results are for DQPSK and QPSK modulation, 2-branch diversity with hard decision decoding, and $CNR = 30$ dB. For MPACS, $f_D = 20$ Hz, $v_1 = 8$, CFO is 5% of the subchannel bandwidth, and timing offset is within one sampling interval.

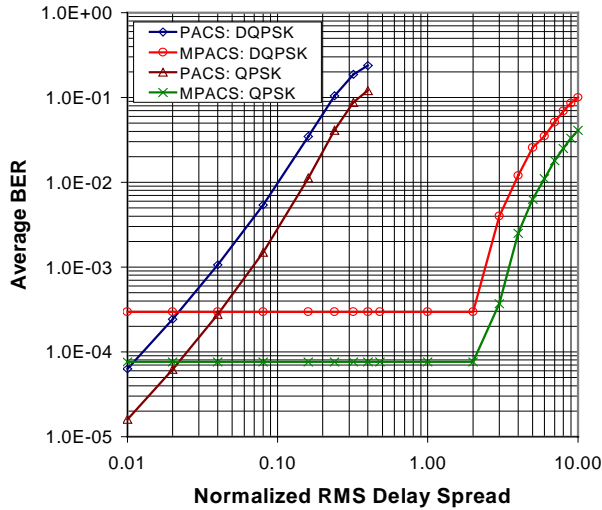


Figure 6. Comparison of average BER performance for PACS and MPACS (for single timeslot operation) with QPSK and DQPSK modulation, as a function of normalized RMS delay spread, with 2-branch diversity.

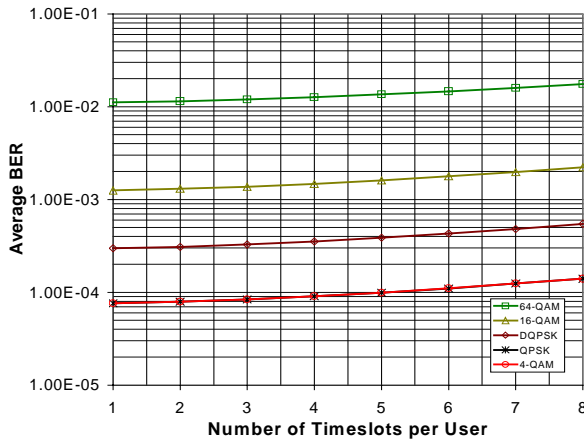


Figure 7. Average BER performance of MPACS for multi-timeslot operation, with QPSK, DQPSK, 4-, 16-, and 64-QAM subcarrier modulation, and 2-branch diversity.

Figure 7 shows the BER performance of MPACS for multi-timeslot operation. The results are shown for QPSK, DQPSK, 4-, 16-, and 64-QAM modulation on each subcarrier, and 2-branch diversity. The $CNR = 30$ dB, $f_d = 20$ Hz, $v_1 = 8$, $\beta_1 = 8$, CFO is 5% of the subchannel bandwidth, and timing offset is within one sampling interval. As expected, QPSK and 4-QAM are identical in their performance, and outperform the others. The performance degrades only slowly with increasing timeslot assignment.

5 Conclusions

In this paper, we investigated the performance of a multicarrier PACS (MPACS) technology that provides a straightforward migration path from the current version of PACS, to support high-speed wireless access. MPACS will be capable of providing high-speed wireless services at nominal user data rates of 32-256 kbps at distances beyond the current range of PACS. For shorter ranges, higher-speed extensions up to 768 kbps are incorporated in the design. The numerical results demonstrate the potential of MPACS to: i) provide improved performance over PACS, ii) provide range extension beyond existing PACS, and iii) support more efficient channelization of the available spectrum.

References

- [1] General Criteria for Version 0.1 Wireless Access Communications Systems (WACS), TR-INS-001313, Issue 1, October 1993, Revision 1, Bellcore, June 1994.
- [2] ANSI J-STD-014B, Personal Access Communication System Unlicensed (Version B) (PACS-UB) Air Interface.
- [3] S. Nahm and W. Sung, "A Synchronization Scheme for Multicarrier CDMA Systems," in *Proc. 4th European Conference on 'Radio Relay Systems'*, Edinburgh, UK, pp. 33-38, Oct. 11-14.
- [4] W. C. Jakes, Ed., *Microwave Mobile Communications*, Wiley, New York, 1974, also reprinted by IEEE Press, in 1994.
- [5] G. L. Stuber and M. Russell, "Terrestrial Digital Video Broadcasting for Mobile Reception Using OFDM," in *Proc. GLOBECOM'95*, pp. 2049-2053.
- [6] J. G. Proakis, *Digital Communications*, 3rd edition, McGraw-Hill, New York, 1995.
- [7] L. E. Miller and J. S. Lee, "BER Expression for Differentially Detected $\pi/4$ DQPSK Modulation," *IEEE Trans. Commun.*, vol. 46, no. 1, pp. 73-81, Jan. 1998.